Fluid dynamic gauging of microfiltration membranes fouled with sugar beet molasses

S.A. Jones [a], Y.M.J. Chew [a], D.I. Wilson [b], M.R. Bird [a,*]

[a] Membrane Applications Laboratory, Department of Chemical Engineering, University of Bath, BA2 7AY, UK
[b] Department of Chemical Engineering & Biotechnology, New Museums Site, Pembroke Street, Cambridge CB2 3RA, UK

ABSTRACT

Fluid dynamic gauging (FDG) was used to track the thickness of the cake layer formed during the microfiltration of a 45° Brix molasses solution using a 1.5 μm polysulphone membrane. A simultaneous measure of flux and deposit thickness throughout the full membrane operating cycle is reported. Asymptotic fouling thicknesses of *ca.* 100 μm are developed after 30 min of filtration. Accordingly, flux declines are severe at *ca.* 93%. Permeate line closed (PLC) operation leads to the complete removal of the deposit layer, and the recovery of 60% of the flux. However, permeate line open (PLO) operation leads to only a 50% flux recovery and an asymptotic deposit thickness of 10 μm. An initial increase and subsequent reduction in flux during chemical cleaning has also been recorded for both acid and alkali cleaning regimes. Effective cleaning regimes for membranes fouled by molasses require an alkali stage followed by an acid stage.

© 2011 Elsevier Ltd. All rights reserved.

1. Introduction

The progressive decline in flux that accompanies the filtration of most food-based liquors necessitates frequent cleaning. Polymeric membrane module configurations (flat sheet and spiral wound) do not readily facilitate back flushing. Thus chemical cleaning remains the membrane regeneration technique of choice. A cleaning agent can affect fouling material present on a membrane surface in three ways: (i) the foulants may be removed by chemical and/or hydraulic interaction, (ii) the morphology of the foulants may be changed (e.g., by swelling or compaction) or (iii) the surface chemistry of the deposit may be altered so that the hydrophobicity or charge is modified (Weis et al., 2003).

In this paper, we report the process of chemical cleaning a microfilter used to treat a 45° Brix molasses solution. Molasses is a thick syrup by-product from the processing of sugar (here, from sugar beet) and contains mainly (i) sugars (sucrose, glucose and fructose), (ii) water, and (iii) inorganic matter (crystalline and dissolved calcium sulphate, calcium oxalate monohydrate and calcium oxalate dihydrate). Microfiltration (MF) offers the possibility of separating the crystalline material (retained in the retentate) from the sugar and divalent ionic species (passed through to the permeate stream). This is of commercial relevance, as the clarification of molasses protects downstream processes such as precipitation and chromatography (Jones et al., 2010).

The cleaning process was investigated in two stages. The first stage was to optimise the cleaning in terms of operating conditions and chemical sequences. The second stage was to use fluid dynamic gauging (FDG) to track the thickness of the cake layer during fouling and its removal rate during cleaning, as an aid to understanding removal mechanisms.

2. Experimental

2.1. Fluid dynamic gauging (FDG)

The principles of the FDG operation are shown schematically in Fig. 1 (Tuladhar et al., 2000). The technique exploits characteristics of the flow of liquid as it is sucked into a nozzle located near a surface. The pressure drop across the nozzle is sensitive to the distance between the nozzle and the surface, h, so that h may be obtained from knowledge of this pressure difference and the flow rate. By combining this with a suitable displacement measurement to gauge the location of the underlying membrane surface, h_o, the deposit layer thickness, δ, can be determined from $\delta = h_o - h$. Any changes in the deposit layer thickness resulting from cleaning or further deposition are monitored. The experimental set-up used in this work is described in detail in Jones et al. (2010).

Nomenclature

d	inside diameter of tube, m	m	discharge mass flow rate, kg/s
d_t	inside diameter of nozzle throat, m	P_i	pressure (gauge) (Pa)
h	clearance between the nozzle tip and gauging surface, m	Δp_n	pressure drop across gauging nozzle, Pa
h_o	clearance between the nozzle tip and clean gauging surface, m	w	width of nozzle rim (m)
J_F	permeate flux, L m^{-2} h^{-1}		*Greek letters*
J_c	PWF flux after cleaning, L m^{-2} h^{-1}	δ	deposit thickness, m
J_r	flux recovery, L m^{-2} h^{-1}	δ_o	initial deposit thickness, m
J_w	PWF flux before fouling, L m^{-2} h^{-1}	α	angle of the nozzle (°)

Lister et al. (2011) reported the successful use of FDG to investigate particulate deposition of glass ballotini onto cellulose ester MF membranes under pressures of up to 64 mbar. In this paper, the FDG is used to investigate fouling under more challenging cross flow and transmembrane pressure conditions for the filtration of a food-based liquor. Results are reported for molasses solutions recycled through the module containing an MF membrane at a cross flow velocity of 1.89 m s^{-1}, 1 bar transmembrane pressure (TMP), and 50 ± 0.5 °C. The permeate flow was collected and plotted versus time. In a calibration test, the gauging flow rate, m, was maintained constant for each condition investigated. The nozzle approached the membrane with h/d_t changing from 1 to 0. Both Δp_{14} and permeate flux were recorded at regular distances from the membrane surface. The subscripts on pressure drop symbols relate locations as shown in Fig. 1. Jones et al. (2010) provide additional information on the calibration method along with an example of a calibration chart. The nozzle must be located within the working range, $h/d_t \leqslant 0.25$, for the gauge to detect the surface reliably. The thickness of a cake layer was determined by measuring Δp_{14} at a fixed value of m: this, together with the corresponding calibration chart yields the new h value. The thickness measurements were performed at intervals of approximately 100 s and each measurement took about 10 s. When measurements were not being made, the gauge was withdrawn from the channel, and the gauging flow stopped to minimise any effect of suction upon the build-up of the cake layer. Removal of the cake layer was also monitored during the subsequent rinsing and cleaning stages.

2.2. Feed, membrane, filtration apparatus and cleaning agents

The cross-flow microfiltration feedstock was sugar beet molasses, provided by *Nordzucker*, Nakskov, Denmark, diluted to the required final mixture with reverse osmosis (RO) water at ambient temperature. A feed volume of 25 l was heated to the desired temperature. The polymeric membranes tested were 0.5, 0.9 and 1.5 μm pore size polysulphone (Psf); *Alfa Laval* (codes GRMRT5, PSURT1, GRTRT8 for the 0.5, 0.9 and 1.5 μm pore sizes respectively). A flat sheet stainless steel membrane module was employed; consisting of five identical channels of width 10 mm, depth 5 mm and length 192 mm (total area available for filtration was 0.0096 m^2). Further details are given in Jones et al. (2010, 2011). The molasses fouled membranes were cleaned using varying concentrations of citric acid (0.1, 0.25, 0.5 wt.%) and sodium hydroxide (0.1, 0.25, 0.5 wt.%) (both chemicals were supplied by *Fisher Scientific*).

2.3. Experimental filtration protocol

Table 1 details the standard conditions employed in the fouling and cleaning stages. These steps represent one complete cycle, except for conditioning which is an additional step for the virgin membrane. Pure water was used for conditioning, removing the glycerine preservative present on new membranes. Weis et al. (2005) found that a water temperature of 60 °C was sufficient to reduce the viscosity of the glycerine and facilitate its removal. Pure water flux (PWF) measurements were taken before fouling, after fouling, and after each cleaning cycle. The fouling flux and cleaning flux measurements were also recorded. All experimental results presented are the average of triplicated runs. The statistical error values were calculated using the average and the standard deviation for the appropriate data sets.

2.4. Chemical cleaning conditions

The cross flow velocity (CFV), temperature and the transmembrane pressure were optimised for all stages of the cleaning cycle. Alkali and acid cleaning was evaluated in terms of the observed flux recovery for the Psf membranes. The cleaning efficiency was
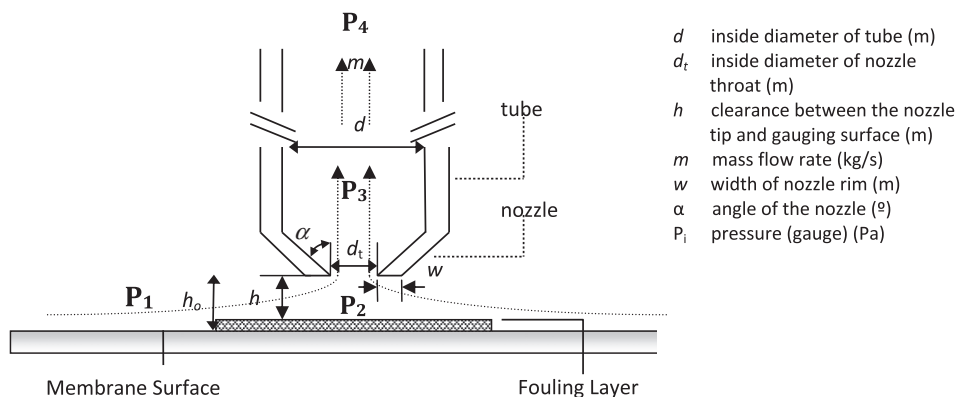

d	inside diameter of tube (m)
d_t	inside diameter of nozzle throat (m)
h	clearance between the nozzle tip and gauging surface (m)
m	mass flow rate (kg/s)
w	width of nozzle rim (m)
α	angle of the nozzle (º)
P_i	pressure (gauge) (Pa)

Fig. 1. Schematic of a typical gauging nozzle showing dimensions (after Chew et al., 2007).

Table 1
Summary of the filtration cycle conditions.

Stage	Fluid	Protocol
Conditioning	Reverse osmosis water	60 °C, 120 min, 1.0 bar, 1.89 m s⁻¹
PWF measurements	Reverse osmosis water	22 °C, 10 min, 1.0 bar, 1.89 m s⁻¹
Fouling	Molasses	60 °C, 90 min, 3.0 bar, 1.89 m s⁻¹
PWF after fouling	Reverse osmosis water	22 °C, 10 min, 1.0 bar, 1.89 m s⁻¹
Rinsing	Reverse osmosis water	22 °C, 15 min, 1.0 bar, 1.89 m s⁻¹
PWF after rinsing	Reverse osmosis water	22 °C, 10 min, 1.0 bar, 1.89 m s⁻¹
Cleaning 1	NaOH/citric acid (conc. varied)	50 °C, 30 min, 1.0 bar, 1.89 m s⁻¹
Cleaning 2	NaOH/citric acid (conc. varied)	50 °C, 30 min, 1.0 bar, 1.89 m s⁻¹
Cleaning 3	NaOH (conc. varied)	50 °C, 30 min, 1.0 bar, 1.89 m s⁻¹
PWF after cleaning	Reverse osmosis water	22 °C, 10 min, 1.0 bar, 1.89 m s⁻¹

evaluated by the ratio of the pure water flux after cleaning (J_c) to the pure water flux measured before fouling (J_w) for each cleaning stage. The percentage flux recovery (%J_r) was defined as:

$$\%J_r = \left(\frac{J_c}{J_w}\right) \times 100 \qquad (1)$$

Twelve treatment protocols were evaluated, comprising of (i) alkali then acid, (ii) acid then alkali and (iii) alkali/acid/alkali steps. Concentrations of 0.1 and 0.25 wt.% were tested for both NaOH and citric acid cleaning agents.

2.5. Scanning electron microscopy

Scanning electron microscopy (SEM) was applied to observe the state of membrane surface after different fouling processes and subsequent cleaning. Air and vacuum-dried membranes were stuck to SEM stubs with conductive paste, followed by coating with a thin layer of gold. Afterwards, the specimens were viewed with a JSM 6310 SEM in combination with a microanalysis system, LINK AN10000 (Oxford Instruments, Abingdon, Oxfordshire, UK). An X-ray Diffractometer will be used to identify and characterise any minerals on the membrane surface.

3. Results and discussion

3.1. Filtration flux behaviour

The 0.5, 0.9 and 1.5 μm Psf membranes were fouled by filtering a 45° Brix molasses solution under the conditions described above.

The 0.5 μm membranes produced a fouling flux of 35 (±2) l m⁻² h⁻¹. The 0.9 μm produced a similar fouling flux of 37 (±2) l m⁻² h⁻¹. Nordzucker (2008) reported that the crystals in the Molasses are *ca.* 1–6 μm wide and 5–20 μm long. These crystals caused the filtration of the Molasses unpractical with the two smaller pore size membranes. The 1.5 μm Psf membranes were the preferred membranes for this study with fouling fluxes of 56 (±3) l m⁻² h⁻¹ and acceptable solids removal. For all cleaning experiments the flux data were normalised, with the initial pure water flux (PWF) taken as 1.0, and the other data scaled accordingly for each protocol. The average initial PWF for the 1.5 μm Psf membranes was 920 l m⁻² h⁻¹. For all cleaning experiments the molasses feed was filtered until it reached the same normalised steady state flux (error ± 6%). The steady state flux was approximately 7% of the initial flux value after 60 min.

3.2. Effect of cleaning operating conditions

Membrane cleaning efficiency is determined by several factors such as the hydrodynamic conditions in addition to the concentration and temperature of the cleaning solution. The sequence of the cleaning steps is also critical (Liu et al., 2000; Chen et al., 2003). In this work, cleaning conditions have been optimised by varying concentration, transmembrane pressure (TMP) and temperature. The TMP pressures tested were 0.5, 1.0 and 2.0 bar whilst maintaining a constant acid and alkali concentration of 0.25 wt.%, a cross flow velocity (CFV) of 1.89 m s⁻¹, and a temperature of 50 °C for a time of 30 min. The optimal TMP for pure water flux recovery after alkali cleaning was 1 bar with a flux recovery of
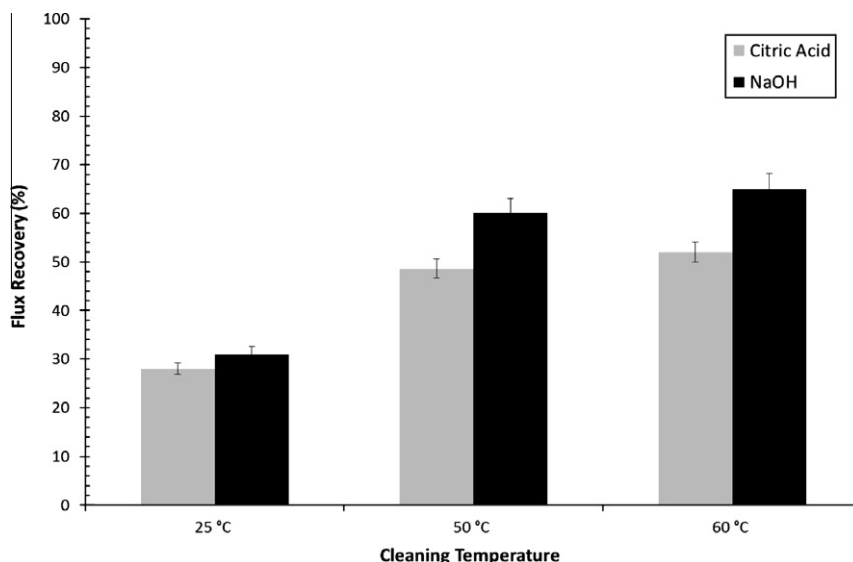

Fig. 2. Comparison of the effect of varying cleaning agent temperature on the average % PWF recovery following fouling and cleaning steps. Conditions: citric acid and NaOH concentrations of 0.25 wt.%, CFV 1.89 m s⁻¹, TMP 1 bar for 30 min.

59% compared to 54% (at 0.5 bar) and 50% (at 2.0 bar). The trend was identical for acid cleaning with an increased flux recovery of 51% (at 1.0 bar) compared to 48% (at 0.5 bar) and 44% (at 2.0 bar). However, the uncertainty in the flux measurements is ±3%, meaning that there is no statistically significant difference in the values recorded. Further experiments are required to reduce the magnitude of the current errors, and see if the trends observed are statistically valid. If so, it is then possible that the low TMP values do not force sufficient cleaning agent through the pores to facilitate cleaning, whilst excessive pressure forces foulants further into the porous structure.

The temperature was varied for the case of constant acid and alkali concentrations of 0.25 wt.%, (CFV 1.89 m s^{-1}; TMP 1 bar) for 30 min. At this stage, three cleaning temperatures were chosen: 22, 50 and 60 °C. Previous work in our labs (Weis et al., 2003; Evans et al., 2008) found that 50 °C is the ideal temperature for cleaning membranes fouled with a wide range of food and bioproducts. The lower and higher temperatures were thus selected to facilitate a meaningful comparison (Fig. 2).

The cleaning fluxes increased noticeably with increasing temperature from 22 to 50 °C. This is most likely to be due both to an increase in the cleaning reaction kinetics at the higher temperature. The results obtained for temperatures of 50 and 60 °C are similar. It was therefore concluded that it was preferable to use the lower temperature of 50 °C for all further cleaning experiments when filtering molasses.

Fig. 3 shows the effect of acid and alkali concentration on PWF recovery after fouling and cleaning. Cleaning with water alone is shown to be insufficient in terms of subsequent PWF recovery, achieving a PWF recovery of only 14%. The lowest concentration

of citric acid tested (0.1 wt.%) lead to the highest PWF recovery recorded, a value of 52%, although this value was not statistically different from the other recovery values recorded for 0.25 and 0.5 wt.%. The NaOH concentration variation experiments were also inconclusive for the range evaluated; the PWF recoveries were similar. The lower concentrations tested (0.1 or 0.25 wt.%) are therefore preferable. Bansal et al. (2006), Bird and Bartlett (2002) and Popović et al. (2009) also found that an increase in concentration of NaOH solution did not always increase flux recovery. The increasing concentration of the acid and alkali solutions could cause the lower flux recovery by; (i) sealing the surface of the deposit and preventing its removal, and/or (ii) inducing gelation when the cleaning solution was introduced (Bansal et al., 2006; Fryer, 1997; Mercadé-Prieto et al., 2010). A lower concentration is therefore preferable both environmentally and economically.

3.3. Efficiency of acid/alkali cleaning sequences

For effective cleaning, molasses deposits require both acid and alkali treatments. The sequence of applying cleaning agents has been investigated and discussed for different feeds by previous authors. Most cleaning regimes consist of an alkali step followed by an acid step (D'Souza and Mawson, 2005). However, in some cases an acid solution has been recommended as the first step, particularly where mineral fouling may be present (Trägårdh, 1989; Daufin et al., 1991). It is also common to follow an alkali then acid step with a second alkaline clean to give a three stage cleaning process. Trägårdh (1989) found that this second alkali clean improved the flux recovery further. This study focuses on testing the three different cleaning sequence options detailed above. Table 2 shows
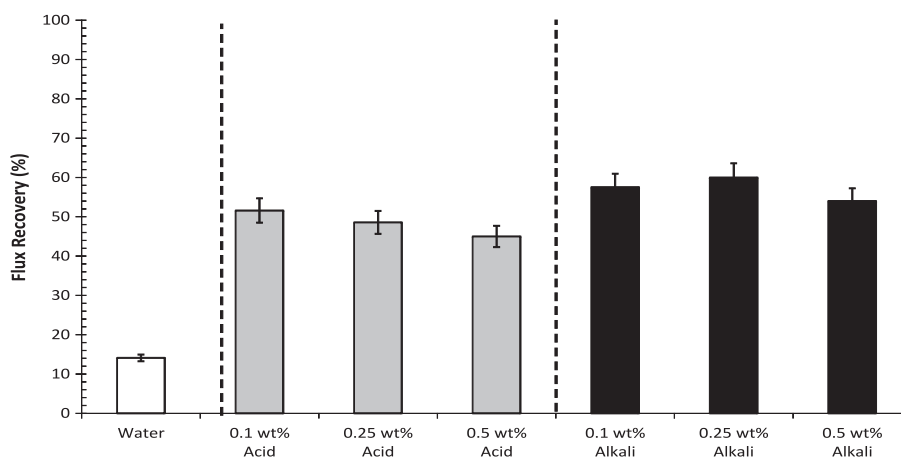

Fig. 3. Effect of citric acid and NaOH (alkali) cleaning agent concentrations on PWF flux recovery after fouling and single-stage cleaning.

Table 2
Cleaning sequences and corresponding observed flux recoveries.

Treatment number	NaOH (wt.%)	Recovery (%)	Citric Acid (wt.%)	Recovery (%)	NaOH (wt.%)	Recovery (%)	Pure water flux recovery (%)
T1	0.10	59	0.10	85			86
T2	0.25	58	0.25	77			77
T3	0.25	60	0.10	83			89
T4	0.10	56	0.25	83			80
T5			0.10	51	0.10	73	69
T6			0.25	50	0.25	79	76
T7			0.25	48	0.10	70	68
T8			0.10	52	0.25	76	69
T9	0.10	59	0.10	85	0.10	65	67
T10	0.25	60	0.10	83	0.25	57	60
T11	0.10	56	0.25	83	0.10	67	67
T12	0.25	58	0.25	77	0.25	62	66

the twelve different cleaning sequences that were tested and the relevant flux recoveries at each cleaning stage.

Fig. 4 shows the final PWF recovery at the end of the cleaning cycle. The first band of treatments (T1–T4) for cleaning with NaOH followed by citric acid gave the higher PWF recovery values (77–89%). From these four, the treatments with the lowest concentration of acid tested (0.1 wt.%) yielded the highest flux recoveries overall (T1 and T3). The addition of a subsequent alkali cleaning step, in T9–T12, resulted in a reduction in the flux obtained and is therefore not preferred.

3.4. Scanning electron microscopy (SEM) images

The morphology of fouled deposits on membrane surfaces for a range of different conditions was inspected using SEM; a selection of which are presented in Fig. 5. Fig. 5(a) and (b) are cross-sections through the asymmetric membrane structure. An active layer of *ca.* 50 μm is clearly visible in Fig. 5(a). The fouled membrane (Fig. 5(b)) shows pore blockage, but mainly surface fouling, confirming the suitability of FDG for studying the process. X-ray diffraction was used to identify the elements present. The deposits
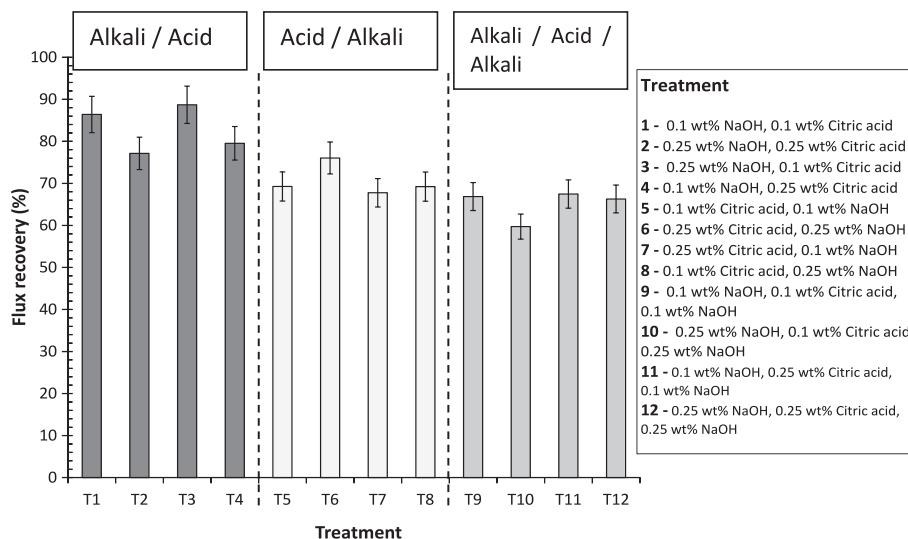

Fig. 4. Effect of citric acid and NaOH (alkali) cleaning sequences on PWF flux recovery after fouling and cleaning.
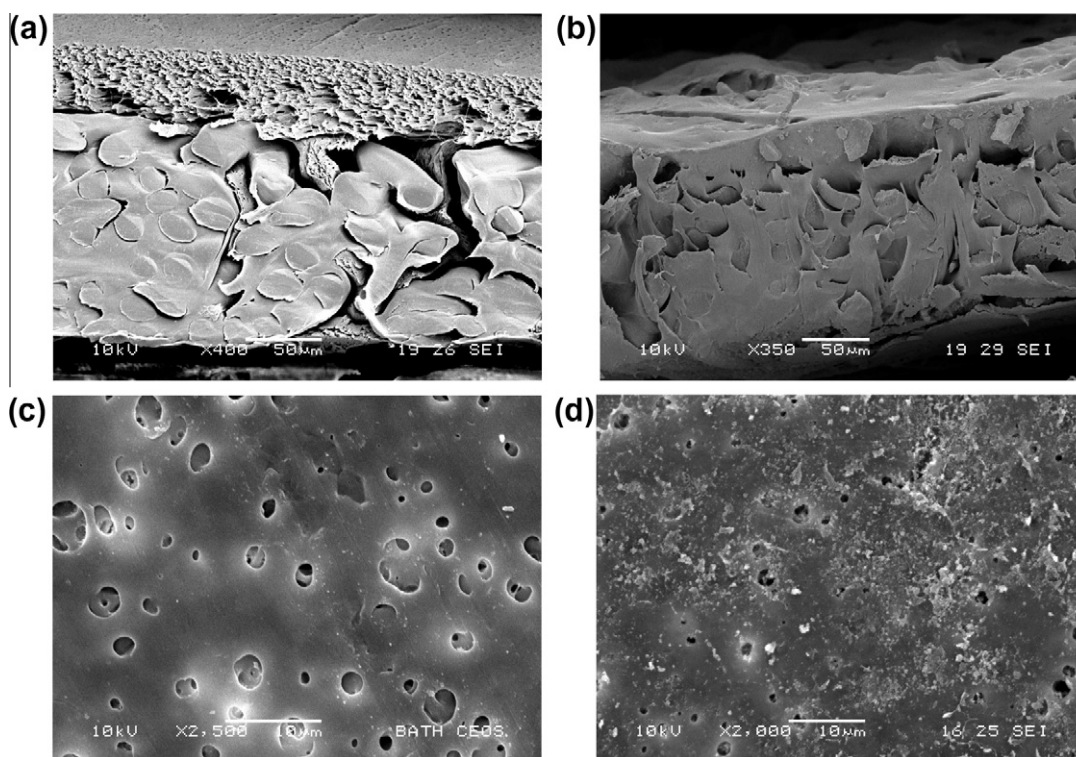

Fig. 5. Scanning electron micrographs of fouling deposits on 1.5 μm Psf membranes. (a) Cross section of a virgin membrane; active layer (feed side) on top, (b) cross section of a fouled membrane; active layer (feed side) on top, (c) surface view of a conditioned virgin membrane, 2500×, and (d) surface view of a fouled membrane, 2000×.

were found to contain calcium, sulphur and oxygen. Whilst the sulphur detected could have come from the Psf membranes, X-ray analysis of molasses filtration deposits obtained in our laboratory using fluoropolymer membranes (i.e. membranes containing no sulphur) also confirmed that sulphur was present in the foulant. The fouling deposits are most likely to be crystals of calcium sulphate, calcium oxalate dihydrate, and calcium oxalate monohydrate. Nordzucker (2008) reported that such crystals are *ca.* 1–6 μm wide and 5–20 μm long. Fig. 5(d) shows fouled membrane surfaces covered with many aggregates in the size range *ca.* 1–6 μm, smaller than those reported by Nordzucker (2008).

3.5. Cake layer removal

FDG was used to investigate the amount of fouling deposit (cake layer) and the subsequent removal occurring during cleaning. Two possible methods of FDG operation during chemical cleaning were considered: (i) Method 1 – permeate side open with recycle back to the feed tank, and (ii) Method 2 (also with recycle to the feed tank) – permeate side closed during the first part of the protocol. Method 1 generates flux data, allowing the calculation of membrane resistances during the cleaning period. In Method 2, cleaning took place with the permeate line closed for 15 min and then opened for the final 15 min. Fig. 6(a) and Fig. 6(b) show the comparison of alkali and acid cleaning with the permeate line open or closed on the removal of the cake layer after fouling with 45° Brix molasses. Removal of the deposits can be facilitated by two different but synergistic mechanisms; (i) shearing effects created by the flow of cleaning agent and (ii) chemical dissolution of the deposits (Bansal et al., 2006).

The cleaning efficiency with the permeate side open was found to be lower than when it was closed. This was also reported by
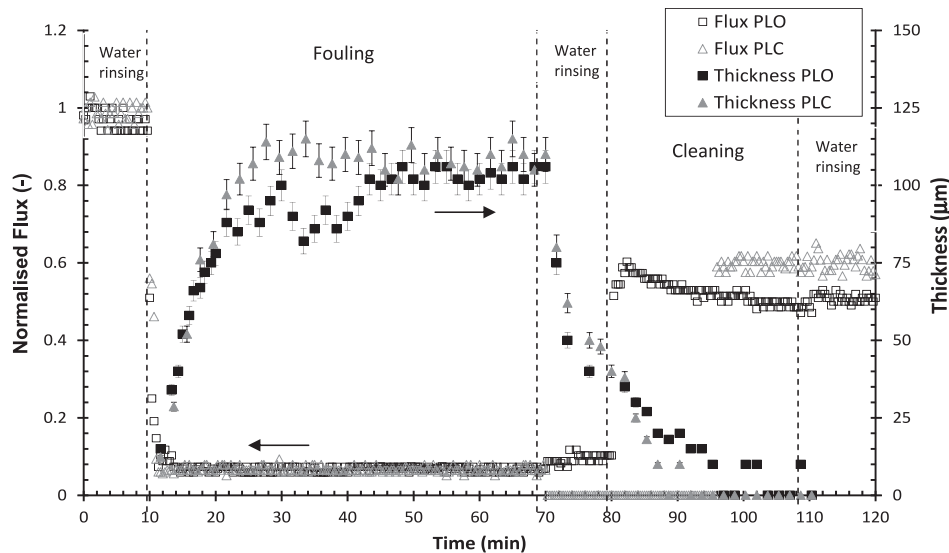

Fig. 6a. Comparison of 0.1 wt.% NaOH cleaning with the permeate line open (PLO) or closed (PLC) during removal of the cake layer following fouling with 45° Brix molasses using 1.5 μm Psf membranes. Open symbols – flux, solid symbols – thickness. Average initial flux; PLO: 894 l m^{-2} h^{-1}, PLC: 925 l m^{-2} h^{-1}. Fouling temperature 60 °C. Cleaning agent temperature 50 °C.
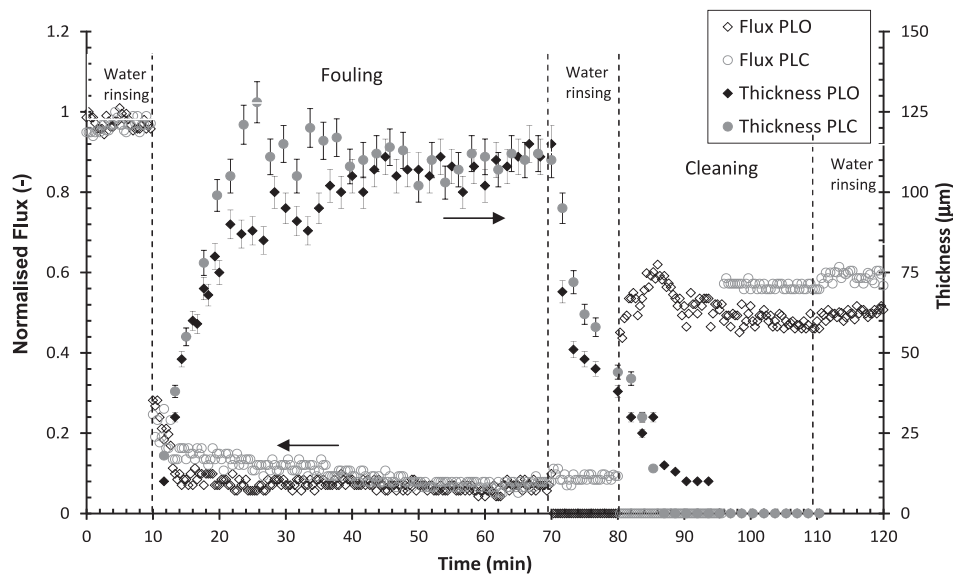

Fig. 6b. Comparison of 0.1 wt.% citric acid cleaning with the permeate line open (PLO) or closed (PLC) during removal of the cake layer following fouling with 45° Brix molasses using 1.5 μm Psf membranes. Open symbols – flux, solid symbols – thickness. Average initial flux; PLO: 918 l m^{-2} h^{-1}, PLC: 927 l m^{-2} h^{-1}. Fouling temperature 60 °C. Cleaning agent temperature 50 °C.
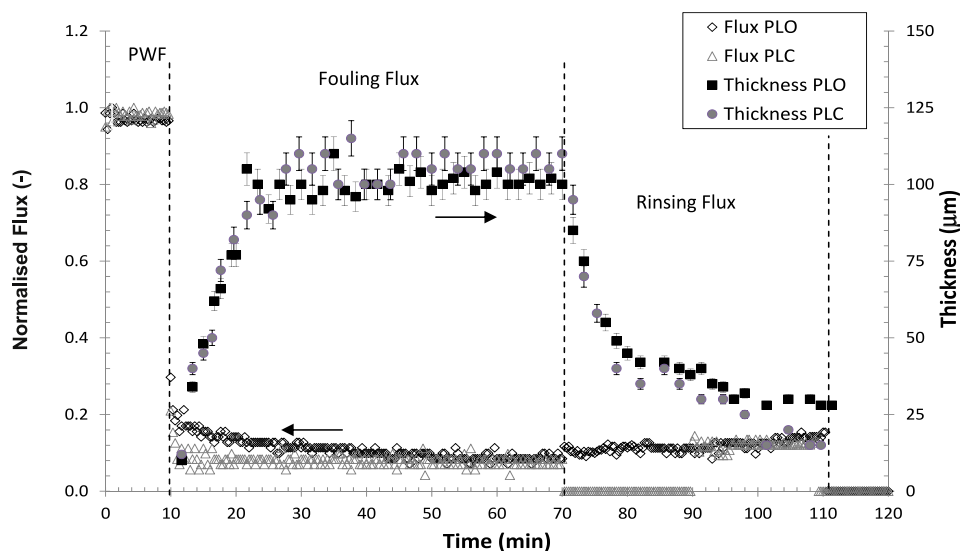
Fig. 7. Effect of permeate line open or closed during rinsing with water alone on removal of the cake layer formed after fouling with 45° Brix molasses using 1.5 µm Psf membranes. Open symbols – flux, solid symbols – thickness. Average initial flux; PLO: 913 l m^{-2} h^{-1}, PLC: 928 l m^{-2} h^{-1}. Fouling temperature 60 °C. Rinsing temperature 22 °C.

Bartlett (1998) when cleaning proteinaceous deposits from MF membranes. This phenomena is also regularly observed in industry for cleaning tubular ceramics – hence the common practice of ensuring that the first stage of any membrane cleaning process be carried out with the permeate line closed, to rinse off deposits rather than force them into the structure, an outcome which is possible when cleaning with the permeate line open.

For all conditions tested the flux increased within the first few minutes of chemical cleaning. After this rise the cleaning flux decreased slightly for the remaining time. This rise in flux could be due to the removal of the loosely bound fouling material from the cake layer, whereas the decrease in flux thereafter could be associated with the swelling of in-pore fouling. Bartlett et al. (1995) and Popović et al. (2009) also reported this decreasing trend in flux, stating that it could be associated with the presence of more tightly bound deposits within the pores undergoing morphological changes (particularly swelling) during the cleaning. This process was modelled by Bird and Bartlett (2002), in terms of the unsteady state hydraulic resistance variation of cake and in-pore foulants.

Fig. 6(a) and Fig. 6(b) also show that during the rinsing stage of the filtration process *ca.* 65% of the cake layer is removed by the application of water alone. However, the removal of *ca.* 65% of cake layer only leads to a PWF recovery of *ca.* 10%, which indicates that the bulk of the resistance to permeate flow, and much of the fouling is likely to be in-pore, and not removed by water rinsing. The role of rinsing in preparing the membrane for the subsequent chemical cleaning step is critically important, as the removal of as much of the deposited layer as possible during rinsing can maximise the efficiency of the cleaning process in terms of time and cleaning agent reduction (Matzinos and Alvarez, 2002).

A further experiment was performed (Fig. 7) to evaluate if it was possible to remove the cake layer completely and restore the PWF values by rinsing with water only. The rinsing efficiency achieved was less than 15% in terms of flux recovery and chemical cleaning was still required. Nevertheless, rinsing did remove 72% (PLO) and 86% (PLC) of the molasses cake layer after 40 min. Rinsing with the permeate line open lead to an asymptotic deposit thickness of *ca.* 25 µm after 40 min of rinsing. By comparison, rinsing with the permeate line closed lead to a deposit thickness of 15 µm after 40 min of rinsing. This thickness value was still

decreasing with time, indicating that further experiments are required to determine whether complete removal of the deposit may be possible by water rinsing alone, if sufficient time is allowed.

4. Conclusions

By optimising a two stage cleaning process, optimal temperature and concentrations were identified for the MF of a 45° Brix molasses solution. Fluid dynamic gauging was successfully used to simultaneously track the thickness of the fouled cake layer and permeate flux during deposition, rinsing and cleaning cycles. A particular advantage of the FDG technique is its ability to determine the thickness of fouling layers where other techniques would find difficulty. For example, the layers formed in this study were opaque, and consequently the determination of the development of deposit thickness with time would have been very challenging using conventional optical microscopy techniques.

The results elucidate the common industrial practice of cleaning with the permeate line closed to aid removal of cake deposits. Asymptotic fouling thicknesses of *ca.* 100 µm were developed after 30 min of filtration. Accordingly, flux declines were severe at *ca.* 93%. Cleaning with the permeate line closed (PLC) is preferable to cleaning with the permeate line open (PLO). PLC operation leads to the complete removal of the deposit layer, and the recovery of 60% of the flux (implying that there are still significant in-pore bound foulants present). However, PLO operation leads to only a 50% flux recovery and an asymptotic deposit thickness of 10 µm.

Effective membrane cleaning protocols following molasses filtration to remove both cake and in-pore bound deposition require both alkali and acid cleaning steps. The best cleaning regime from the set tested achieved a pure water flux recovery of 89% using an NaOH concentration of 0.25 wt.% followed by a stage using 0.1 wt.% citric acid.

An initial increase and subsequent reduction in flux during chemical cleaning has also been recorded for both acid and alkali treatments. This supports previous membrane cleaning findings for the removal of food based foulants based on the simultaneous removal of the cake and the swelling of in-pore bound deposition (Bird and Bartlett, 2002).

Acknowledgements

References

Bansal, B., Al-Ali, R., Mercadé-Prieto, R., Chen, X.D., 2006. Rinsing and cleaning of α-lactalbumin fouled MF membranes. Separation and Purification Technology 48, 202–207.

Bartlett, M., 1998. Chemical cleaning of fouled membrane systems, Doctoral Dissertation Chemical Engineering Department, University of Bath.

Bartlett, M., Bird, M.R., Howell, J.A., 1995. An experimental study for the development of a qualitative membrane cleaning model. Journal of Membrane Science 105, 147–157.

Bird, M.R., Bartlett, M., 2002. Measuring and modelling flux recovery during the chemical cleaning of MF membranes for the processing of whey protein concentrate. Journal of Food Engineering 53, 143–152.

Chen, J.P., Kim, S.L., Ting, Y., 2003. Optimization of membrane physical and chemical cleaning by a statistically designed approach. Journal of Membrane Science 219, 27–45.

Chew, Y.M.J., Paterson, W.R., Wilson, D.I., 2007. Fluid dynamic gauging: a new tool for studying deposition on porous surfaces. Journal of Membrane Science 296, 29–41.

Daufin, G., Merin, U., Labbé, J.P., Quémerais, A., Kehervé, F.L., 1991. Cleaning of inorganic membranes after whey and milk ultrafiltration. Biotechnology and Bioengineering 38, 82–89.

D'Souza, N.M., Mawson, A.J., 2005. Membrane cleaning in the dairy industry: A review. Critical Reviews in Food Science and Nutrition 45, 125–134.

Evans, P.J., Bird, M.R., Pihlajamaki, A., Nystrom, M., 2008. The influence of hydrophobicity, roughness and charge upon ultrafiltration membranes for black tea liquor clarification. Journal of Membrane Science 313, 250–262.

Fryer, P.J., 1997. Thermal treatment of foods. In: Fryer, P.J., Pyle, D.L., Rielly, C.D. (Eds.), Chemical Engineering for the Food Industry. Blakie Academic and Professional, London, pp. 331–382.

Jones, S.A., Chew, Y.M.J., Bird, M.R., Wilson, D.I., 2010. The application of fluid dynamic gauging in the investigation of synthetic membrane fouling phenomena. Food and Bioproducts Processing 88, 409–418.

Jones, S.A., Bird, M.R., Pihlajamki, A., 2011. An experimental investigation into the pre-treatment of synthetic membranes using sodium hydroxide solutions. Journal of Food Engineering 105, 128–137.

Lister, V.Y., Lucas, C., Gordon, P.W., Chew, Y.M.J., Wilson, D.I., 2011. Pressure mode fluid dynamic gauging for studying cake build-up in crossflow microfiltration. Journal of Membrane Science 336 (1–2), 304–313.

Liu, C., Caothien, S., Hayes, J., Caothuy, T., 2000. Membrane chemical cleaning: from art to science, Scientific and Laboratory Services, Pall Corp.

Matzinos, P., Alvarez, R., 2002. Effect of ionic strength on rinsing and alkaline cleaning of ultrafiltration inorganic membranes fouled with whey proteins. Journal of Membrane Science 208, 23–30.

Mercadé-Prieto, R., Gunasekaren, S., Paterson, W.R., Wilson, D.I., 2010. Fundamentals of model protein gel dissolution: the path to elucidating industrial dairy cleaning. In: Fouling & Cleaning in Food Processing. Jesus College Cambridge, UK, pp. 190–198 (22–24th March 2010).

Nordzucker, 2008. Personal Correspondence; Composition of Insoluble Solids in Molasses. Nordzucker, Nakskov.

Popović, S.S., Tekić, M.N., Djurić, M.S., 2009. Kinetic models for alkali and detergent cleaning of ceramic tubular membrane fouled with whey proteins. Journal of Food Engineering 94, 307–315.

Trägårdh, G., 1989. Membrane cleaning. Desalination 71, 325–335.

Tuladhar, T.R., Paterson, W.R., Macleod, N., Wilson, D.I., 2000. Development of a novel non-contact thickness measurement technique for soft deposits and its application in fouling studies. Canadian Journal of Chemical Engineering 78, 935–947.

Weis, A., Bird, M.R., Nystrom, M., 2003. The chemical cleaning of polymeric UF membranes fouled with spent sulphite liquor over multiple operational cycles. Journal of Membrane Science 216, 67–79.

Weis, A., Bird, M.R., Nyström, M., Wright, C., 2005. The influence of morphology, hydrophobicity and charge upon the long-term performance of ultrafiltration membranes fouled with spent sulphite liquor. Desalination 175, 73–85.